Journal of Structural Geology, Vol. 2, No. 3, pp. 311 to 316.
Pergamon Press Ltd. 1980. Printed in Great Britain

Classification of fold interference patterns: a reexamination

R. L. THIESSEN and W. D. MEANS

Department of Geological Sciences, State University of New York at Albany, 1400 Washington Avenue, Albany, NY 12222, U.S.A.

(*Received* 22 *October* 1979; *accepted* 29 *January* 1980)

Abstract—A modification of Ramsay's (1967) classification of fold interference patterns is proposed, based upon angular parameters in part different from those used by Ramsay. We use the angle between the axes of the first folds and the pole to the axial planes of the second folds as one of our parameters (gamma). Use of this angle plus beta, one of Ramsay's angles, provides a more natural basis for classification of three-dimensional patterns and in particular avoids several ambiguities in Ramsay's scheme.

INTRODUCTION

WHERE two sets of folds of similar length interfere, the layering in rocks assumes complicated three-dimensional forms that are reflected in various two-dimensional interference patterns (Ramsay 1962, 1967). This paper presents a modification and extension of Ramsay's classification of such patterns, and some observations that may be useful to field workers dealing with interference structures. We retain Ramsay's terminology and notation as much as possible and also follow him in considering only those patterns that result from superposing on the first folds, either a shear folding or a shear folding combined with homogeneous flattening. The resulting patterns are thought to sufficiently represent the range of patterns to be encountered in nature, even though natural superposed folding, or synchronous cross-folding, must rarely occur by such simple deformations. The interference patterns figured here were calculated by a computer program described elsewhere (Thiessen, in press). This program permits any number of folding movements to be superposed in any desired relative orientations and the calculation and display of serial, two-dimensional cross-sections in any desired orientation.

REFERENCE AXES AND INTER-AXIAL ANGLES

Following Ramsay (1967, p. 521) we designate the shear direction in the second axial planes a_2 and the direction normal to this in the axial planes b_2 (Fig. 1). Poles to the first and second axial planes are designated c_1 and c_2 respectively. The direction of the first fold axis is termed f_1 (Ramsay 1967, fig. 10-2) and the normal to f_1 in the first axial planes is d_1. Where the first folds are assumed to have formed by heterogeneous simple shear on the first axial planes, a_1 and b_1 are respectively the slip direction in the first axial planes and the normal to the slip direction. Notice that a_1 and b_1 describe the movements that produced the first folds, while d_1 and f_1 describe the orientation of the resulting first fold forms. Only in special cases, such as when b_1 lies within the original plane of layering will a_1 be parallel to d_1 or b_1 be parallel to f_1.

Interference effects depend on the orientations of the axes a_2, b_2 and c_2 relative to d_1, f_1 and c_1, or in other words, on the inter-axial angles relating the two sets of axes (Fig. 2). In the analyses of Carey (1962) and Ramsay (1967) only two of these angles are employed, as indicated in Fig. 2. We show below that two angles are, in fact, sufficient for classification of three-dimensional interference patterns, but that the best angles for this purpose are Ramsay's angle β and a new angle we call γ (Fig. 2). For other purposes we retain Ramsay's angle α and introduce another new angle δ. The first three angles are allowed to take values from 0 to +90 degrees.

THE ORIENTATION VOLUME

Various orientations of a_2, b_2 and c_2 relative to d_1, f_1 and c_1 can be represented by points in a cubic volume with

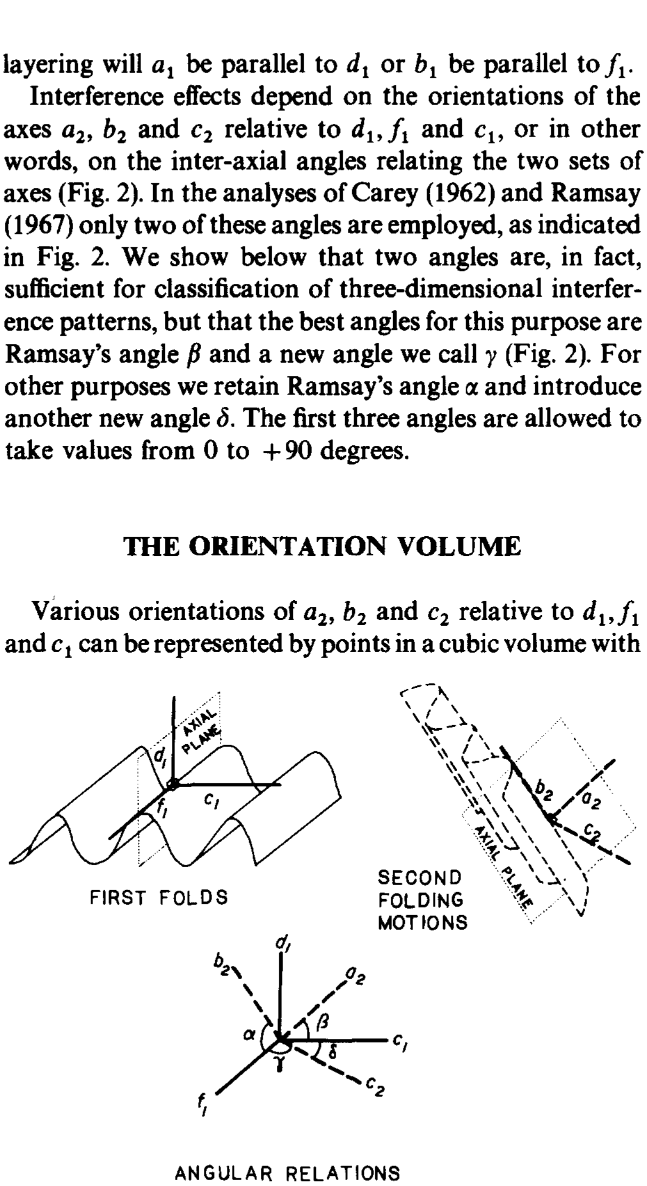

Fig. 1. Axes used to describe the relative orientations of the first folds and the second folding movements. The wave train drawn in solid lines at the left represents real folds in layering after the first movements. The wave train drawn at the right represents imaginary folds formed by the second movements alone (i.e. in a dyke injected normal to a_2 between the two episodes of folding). Below are shown both sets of axes and the angles α, β, γ and δ.

	d_1	f_1	c_1
a_2	$a_2 \wedge d_1$ Ⓒ	$a_2 \wedge f_1$	$a_2 \wedge c_1$ β Ⓡ
b_2	$b_2 \wedge d_1$	$b_2 \wedge f_1$ Ⓒ α Ⓡ	$b_2 \wedge c_1$
c_2	$c_2 \wedge d_1$	$c_2 \wedge f_1$ γ	$c_2 \wedge c_1$ δ

Fig. 2. Interaxial angles between a_2, b_2 and c_2 and d_1, f_1 and c_1. In this paper the angles α, β, γ and δ are employed. The angles used by Ramsay (1967) and Carey (1962) are designated by R and C respectively.

α, β and γ plotted parallel to its edges (Fig. 3a). However, not all combinations of α, β and γ are possible. The first constraint is that

$$\alpha + \gamma \geq 90°, \tag{1}$$

since α and γ are measured from two orthogonal lines (b_2 and c_2) to a third line (f_1). Combinations of α and γ failing to satisfy (1) are therefore impossible and this removes from consideration the part of the dashed cube below the plane marked with a solid line in Fig. 3(b). The second constraint arises from the fact that d_1, f_1 and c_1 and a_2, b_2 and c_2 are both orthogonal sets of axes, so that the orthogonality relations (Nye 1964, p. 34) must hold, namely:

$$\cos^2(a_2 \wedge f_1) + \cos^2 \alpha + \cos^2 \gamma = 1,$$

and (2)

$$\cos^2(a_2 \wedge d_1) + \cos^2(a_2 \wedge f_1) + \cos^2 \beta = 1.$$

Setting the left-hand sides equal yields the necessary condition that

$$\cos^2 \alpha + \cos^2 \gamma \geq \cos^2 \beta, \tag{3}$$

since $\cos^2(a_2 \wedge d_1)$ will always be positive or zero. Condition (3) removes from consideration all combinations of α, β and γ lying in front of a curved surface that cuts off the top right corner of the cube (Fig. 3c). The remaining volume (Fig. 3d) is the 'orientation volume' representing possible relative orientations of the first folds and the second folding movements. Ramsay's (1967, p. 531) classification is projected onto the α–β plane of this volume, with γ unspecified.

Points on the surfaces of the orientation volume (except for the point $\alpha = \beta = \gamma = 90$ degrees) represent a single orientation of the axes a_2, b_2 and c_2 relative to d_1, f_1 and c_1. By 'single orientation' we mean one orientation together with all symmetrically equivalent orientations. For each point inside the orientation volume, however, the combination of α, β and γ is consistent with two different (i.e. not symmetrically equivalent) relative orientations of the axes. An example is shown in Fig. 4 in which a_2, b_2 and c_2 are arbitrarily plotted normal and parallel to the plane of the projection. f_1 must lie at the intersection of a small circle of radius α drawn about b_2 and a small circle of radius γ drawn about c_2. There is, of course, another intersection of the two small circles in the lower hemisphere immediately beneath the point marked f_1 in Fig. 4, and indeed another six points with the same α and γ values, at l, m and n (three in each hemisphere), if we take into account that the axes a_2, b_2 and c_2 do not have distinct positive or negative ends. The total of eight f_1 orientations consistent with a single pair of α and γ values are equivalent orientations, and we need consider only one of them. We choose the one marked f_1 in Fig. 4 and draw in an upper hemisphere great circle normal to f_1 (dashed). This plane must contain the directions of c_1 and d_1, arranged so as to form a right-handed orthogonal system. A small circle of radius β about a_2 intersects the dashed great circle in points c_1 and c_1', which are the two orientations of c_1 consistent with the given angles α, β and γ. Notice that c_1 and c_1' are in general differently oriented from each other with respect to the a_2, b_2 and c_2 axes. The angle $\delta(c_2 \wedge c_1)$ is then used to specify one of these orientations. This angle is the angle between the two fold

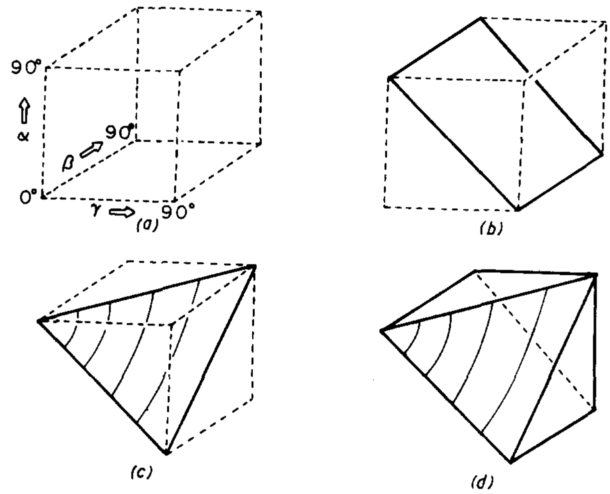

Fig. 3. Diagrams showing the relationship of the orientation volume (Fig. 5) and geometric constraints creating it. See text for details.

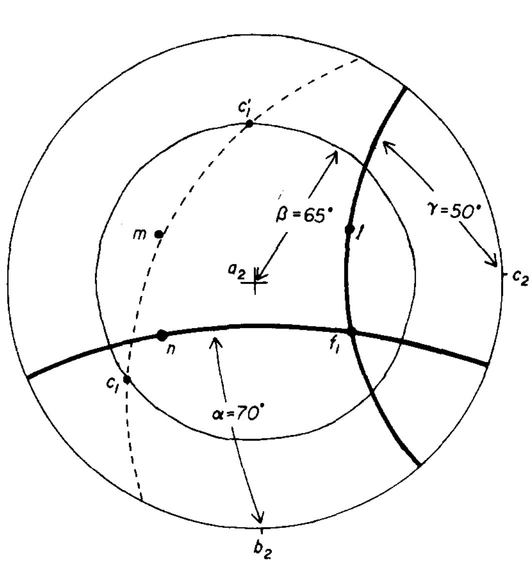

Fig. 4. Upper hemisphere stereographic projection showing the two orientations of c_1 resulting from a single set of α, β, γ values. See text for details.

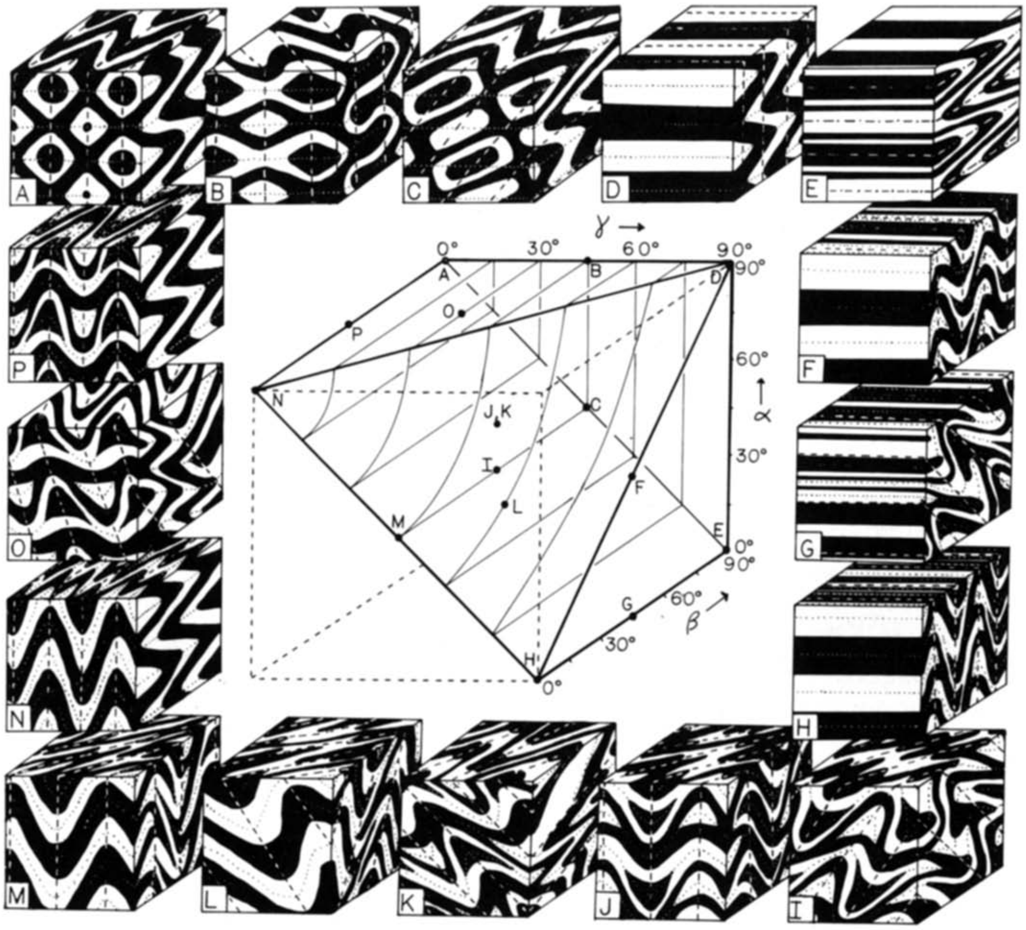

Fig. 5. Orientation volume with representative interference patterns depicted in the surrounding cubes. Cases J and K are represented by points in the interior of the volume; other cases correspond to points on the surface of the volume. In all cases, layering was initially parallel to the front cube face. The first folds resembled case D, with initially horizontal axial planes and fold axes parallel to the bottom front edge of each cube. The second folding motions are sine waves similar in form to those shown in case D, but with varying orientations given by Table 1. First axial planes in their final configuration are shown with dotted lines while second axial planes are shown with dashed lines. The former are omitted on the top faces of cubes I–M for clarity, but these are all W-M shapes with the trace of the first axial planes paralleling the second axial planes, as in case N and Fig. 7.

axial planes measured in the plane of the two poles. δ is related to α, β, γ by

$$\cos\delta = \frac{-B \pm \sqrt{(B^2 - 4AC)}}{2A}, \tag{4}$$

where

$$A = \cos^2\alpha + \cos^2\gamma,$$

$$B = 2\cos\gamma\cos\beta\sqrt{(1 - \cos^2\alpha - \cos^2\gamma)},$$

$$C = \cos^2\beta\sin^2\gamma - \cos^2\alpha.$$

This equation yields one value of δ for all but one point on the outside of the orientation volume, two values for any point inside the volume, and all values of δ (from 0 to 90 degrees) for the special case where $\alpha = \beta = \gamma = 90$ degrees, for which $A = 0$. For points inside the orientation volume we have never found a case where the two different interference patterns, corresponding to the two different δ values, are much different from one another. For many purposes then, the three angles α, β and γ suffice.

Figure 5 shows the orientation volume with representative interference patterns around it (A to P). Each case is represented by a cube. The first folding episode was sinusoidal with a fold axis parallel to the front horizontal cube edge and an axial plane parallel to the top face of the cube. Bedding was initially parallel to the front face. The first fold form can be seen in case D of Fig. 5. The second fold form is the same as the first, but has a different orientation for each cube (Table 1). The first and second fold axial planes are shown with dotted and dashed lines, respectively.

THREE-DIMENSIONAL INTERFERENCE PATTERNS

Three-dimensional interference patterns divide naturally into the four classes recognized by Ramsay (1967, pp. 520–533) and called by him Types 0, 1, 2 and 3. The classes differ from one another in whether material lines and planes along the first fold hinge lines and axial planes remain straight and planar or become folded as a result of the second movements.

The simplest angular criteria for the three-dimensional classes are given in terms of β and γ as shown in Fig. 6. These criteria are easily understood as follows. In hetero-

Table 1. Orientations of second axial planes and b_2 for Fig. 5 cases A–P. In Fig. 5, the top cube faces are assumed to be horizontal with north towards the back of the cube and east to the right. Strikes and trends are measured clockwise from north

	Second axial plane		b_2	
Case	Strike	Dip	Trend	Plunge
A	0°	90°	0°	90°
B	135°	90°	0°	90°
C	0°	45° W	270°	45°
D	90°	90°	0°	90°
E	0°	0°	90°	0°
F	90°	90°	270°	45°
G	90°	45° N	90°	0°
H	90°	90°	90°	0°
I	35°	60° NW	235°	30°
J	45°	90°	225°	45°
K	18°	58° SE	31°	14°
L	59°	73° SE	231°	24°
M	45°	90°	45°	0°
N	0°	90°	0°	0°
O	155°	73° NE	0°	55°
P	0°	90°	0°	45°

geneous simple shear, the pre-existing planes that remain planar are planes lying parallel to the shear direction. c_1 must therefore be perpendicular to a_2 for Types 0 and 1, or in other words β must be 90 degrees. The lines that remain straight, on the other hand, are lines parallel to the shear planes, so f_1 must be perpendicular to c_2 for Types 0 and 3, or $\gamma = 90$ degrees. Where neither of these conditions prevails ($\beta \neq 90$ degrees and $\gamma \neq 90$ degrees) the second movements must fold both the axial planes and the hinge lines of the first folds, and patterns of Type 2 necessarily emerge. The foregoing statements apply equally well where the second movements involve a homogeneous flattening combined with the simple shearing, since a homogeneous flattening cannot introduce curvature in lines and planes.

Type 0 patterns

In the narrow sense, Type 0 patterns are not interference patterns at all, since the first folds remain plane and cylindrical and there is accordingly 'no characteristic pattern of interference' (Ramsay 1967, p. 531) in two-dimensional cross sections of such folds. In a broader sense, however, the usual sense of the word 'interference' in optics, for example, Type 0 patterns are interference patterns despite their simplicity.

We recognize two kinds of Type 0 patterns. The first, which plots in the upper right corner ($\alpha = \beta = \gamma = 90$ degrees) of our orientation volume (Fig. 5, case D) is geometrically trivial and mechanically unlikely. This

	FIRST FOLD HINGE LINES	FIRST FOLD AXIAL PLANES	β	γ
TYPE 0	STRAIGHT	PLANAR	90°	90°
TYPE 1	FOLDED	PLANAR	90°	$\neq$90°
TYPE 2	FOLDED	FOLDED	$\neq$90°	$\neq$90°
TYPE 3	STRAIGHT	FOLDED	$\neq$90°	90°

Fig. 6. Angular criteria necessary for Ramsay's four types of three-dimensional fold interference patterns.

pattern arises where a_2 is parallel to f_1, so that the second folding movements produce no change at all in the form of the first folds. Particles are displaced within the folded surface in the $a_2 = f_1$ direction but the surface itself is not further deformed. The $\alpha = \beta = \gamma = 90$ degrees point of the orientation volume is unique in that one can rotate the second axes about a_2 without any change in α, β and γ while δ varies from 0–90 degrees. There are thus an infinite number of orientations of the two sets of axes with $\alpha = \beta = \gamma = 90$ degrees, none of which produce recognizable interference forms. Here is an example of the inadequacy of a classification scheme based only on angles α and β. We see that where both these angles are 90 degrees patterns of Type 0 can arise, though Ramsay's diagram (1967, p. 531) might lead one to think that $\alpha = \beta = 90$ degrees must lead to Type 1 patterns and his caption indicates that the only values of α and β that lead to Type 0 patterns are $\alpha = 0$ and $\beta = 90$ degrees.

The second kind of Type 0 pattern represented by all points except the top one along the back, right, vertical edge of the orientation volume ($\beta = \gamma = 90$ degrees, $\alpha \neq 90$ degrees) (case E), is the more general kind, where the first folds remain plane cylindrical but their amplitude or wavelength changes and hinge migration may occur. This kind of Type 0 pattern is the most common kind of interference pattern, in the sense that it arises continually in the course of normal progressive folding, if we regard the second movements as simply the next increment of deformation in an extended progressive deformation. There is thus no difference between the study of this kind of Type 0 interference patterns and the study of the purely geometric aspects of fold evolution, but this will not be pursued further.

Type 1 patterns

Ideal Type 1 (basin and dome) patterns arise for orientations that plot on the back triangular face of the orientation volume (Fig. 5, cases A, B and C), except for the right-hand vertical edge where Type 0 patterns occur. Sections cut parallel to the overall orientation of the layering after the second movements show the characteristic basin and dome patterns, with one layer making a continuous network of outcrop where $\gamma + \alpha = 90$ degrees. Except where $\alpha = 90$ degrees, lines of domes or of basins tend to be arranged *en échelon* along the first or second axial plane traces, as pointed out by O'Driscoll (1962, pp. 156–159).

Type 3 patterns

Ramsay's ideal Type 3 patterns occur along the $\alpha = 0$ edge of his diagram (1967, p. 531), which corresponds to the lower right edge of our orientation volume (Fig. 5, cases G and H). However, ideal type 3 patterns can also be formed at other values of α, so long as $\gamma = 90$ degrees (case F). In our diagram then, ideal Type 3 patterns arise for all orientations on the right, vertical, triangular face of the orientation volume, except for its vertical back edge where

Type 0 patterns occur. The distinguishing feature of all Type 3 patterns is that there always exists a family of two-dimensional viewing planes (parallel to f_1) on which the outcrop pattern is made up of parallel straight lines. We call such patterns *linear* patterns. The family of planes on which linear patterns appear is represented by the front and top faces of the blocks in Fig. 5. Viewing planes cut perpendicular to f_1 show the familiar hook pattern along the diagonal $\alpha = \beta$ and more complicated patterns, again with hooks, elsewhere in the $\gamma = 90$ degree plane. Type 0 patterns also display this family of linear patterns, but the perpendicular viewing plane will show a simple wave form. Notice that ideal Type 3 patterns can form at any value of α, so long as $\gamma = 90$ degrees. They are not restricted to situations with α close to zero, as Ramsay's classification tends to suggest (Ramsay 1967, pp. 521–531).

The hook pattern is sometimes taken as diagnostic of Type 3 relations between fold generations ($\gamma \approx 90$ degrees). We show an example shortly of how an ideal Type 2 interference form with $\gamma = 0$ degrees can be sliced to yield hook patterns in certain viewing planes.

If a Type 3 example is formed with very tight folds, it may resemble transposed layering, complete with hooks and apparently discontinuous layers, particularly if the fold limbs are highly attenuated.

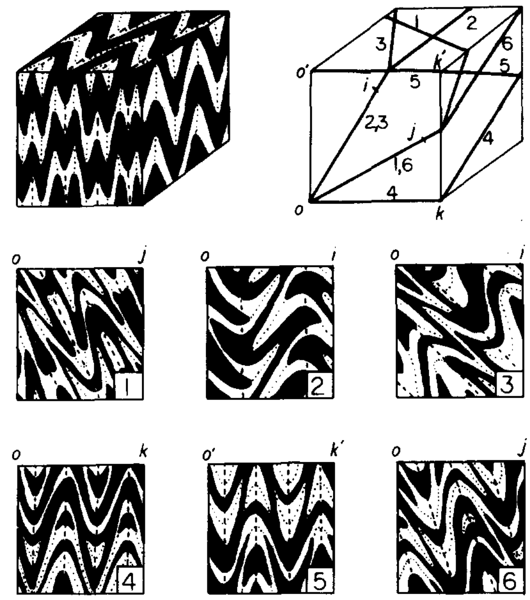

Fig. 7. Variety of two-dimensional patterns arising for different cuts through a type 2 three-dimensional pattern. The top left cube is the same case as Fig. 5, case N ($\alpha = 90°$, $\beta = 0°$, $\gamma = 0°$), but is viewed differently. The top right cube shows orientations of the six planes cut through this case that are represented in the six squares below. It depicts the top, front, and right side of a cube, as in the left-hand cube. Dotted and dashed lines are traces of first and second axial planes respectively. The first folds had vertical axial planes, horizontal hinge lines and a profile section represented by the right-hand face of the cube. The second folds have vertical axial planes parallel to the side of the cube and introduce folds in the first axial planes with a profile shown on the top face of the cube.

Type 2 patterns

Type 2 patterns arise for combinations of α, β and γ plotting in the interior of the orientation volume or on its top or bottom surfaces. One of our aims has been to discover whether there is any natural way to subdivide Type 2 patterns. We have searched in particular for two-dimensional patterns that arise within the Type 2 volume and that are distinctive of various parts of the volume. So far we have had little success in this, partly because Type 2 patterns can be sliced to yield a wide variety of two-dimensional patterns of which Fig. 7 shows an example. The block diagram (Fig. 7, upper left) shows a Type 2 pattern as far as possible from the Type 1 and Type 3 planes of the orientation volume: $\alpha = 90$ degrees and $\beta = \gamma = 0$ degrees (Fig. 5, case N). First folds with vertical axial planes and hinge lines oriented normal to the side of the block diagram have been refolded by shearing on planes parallel to the side of the block in a direction normal to the front of the block. The three faces of the block itself, and the six additional viewing surfaces sliced in various more general orientations through the block, show how a variety of two-dimensional patterns can be associated with a single three-dimensional pattern. Simple sine waves are seen on the side of the block. What might be called 'repeated sine waves' are seen on the top surface where one black layer and one white layer occur repeatedly in the apparent stratigraphy. The front face shows 'W' and 'M' patterns that arise in this orientation whenever the half wavelength of the first folds is less than the amplitude of the second 'folds' (for example, the folds that would have arisen in a dyke injected perpendicular to a_2 between the two folding episodes). In other cuts one sees various symmetric and non-symmetric crescents (4–6) normally associated with Type 2 patterns, as well as arrows (1) and very complex shapes (3), and also hooks (2). It appears that hooks can appear in some sections through most Type 2 patterns, so their existence in a map pattern or exposure surface should not by itself be taken to indicate Type 3 interaxial relations. Similarly, sine wave patterns can appear in sections cut through any Type 1 or Type 2 pattern which are parallel to the second axial plane or the a_2–f_1 plane, and so are not diagnostic of Type 0 patterns.

The only really distinctive two-dimensional patterns we are aware of are those seen in sections that one knows to be cut parallel to the overall attitude of the original layering. In such sections, three-dimensional patterns of Types 0 and 3 show straight lines, Type 1 displays closed rectangles or loops, and Type 2 is characterized by crescents or repeated sine waves. These distinctive patterns repeat on a lattice governed by the wavelengths of the folds and the interaxial angles. The repeated sine wave pattern (e.g. top surface of block, Fig. 7) occurs when a_2 lies parallel to the overall orientation of layering after the first folding. In the orientation volume of Fig. 5 this can occur on or near the top curved surface (cases L, M and N).

Asymmetric first folding

We have calculated a number of interference patterns that arise when the second folding movements are superposed on asymmetrical first folds. The various three-dimensional Types are still easily recognizable and conform to the angular criteria set out in Fig. 6. An interesting situation arises when there are two different orientations of layers present before the first folding, such as bedding and cross-cutting veins, so that two different f_1 orientations can arise although c_1 is the same for both kinds of layers. In this situation (see Fig. 2), β and δ will be the same for both kinds of layers but different values of α and γ may arise for the beds and the veins. This makes it possible for the beds to undergo Type 2 refolding while the veins undergo Type 3, or vice versa. Or the beds could be refolded into a Type 1 basin and dome configuration while the veins develop a simple Type 0 configuration. In the latter case, the veins, with their simple fold forms, might easily be misinterpreted as having been emplaced after the first folding but before the second.

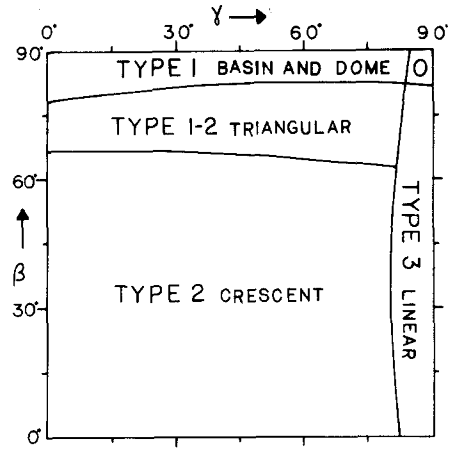

Fig. 8. β–γ projection of the orientation volume, showing regions of the various fold types. Boundaries are gradational. Simple (Type 0) patterns are in the upper right corner and Triangular is a gradational region (1→2).

The β–γ projection

The simplest two-dimensional projection of the orientation volume of Fig. 5 is obtained by viewing it parallel to the α axis. In such a projection, a β–γ projection, all possible patterns of Type 0 plot in one corner, and all possible patterns of Types 1 and 3 plot along two edges of the diagram (Fig. 8). This simple result is not obtained if one views the orientation volume along the γ axis, as Ramsay does in effect in obtaining his α–β projection. Remembering that patterns of Types 0, 1 and 3 plot respectively along the vertical edge and the two vertical bounding planes of the orientation volume, it can be seen from Fig. 5 that an α–β projection of the volume will have patterns of Types 0 and 1 occupying one edge of the projection and patterns of Type 3 spreading over half the area occupied by patterns of Type 2. The β–γ projection contains no such overlaps because it is obtained by projecting parallel to the line in the orientation volume that is common to the Type 1 and Type 3 planes and which also happens to be the Type 0 lines.

In Fig. 8 we have labelled five fields according to the kind of diagnostic two-dimensional patterns that arise and the type of three-dimensional relations that obtain, or approximately obtain. All the boundaries are gradational and vary about ± 5 degrees as α varies. Patterns of basin and dome type with oval or four-sided outcrop patterns are characteristic of situations with very high values of β. With decreasing β these patterns grade, through a field with triangular closed outcrop patterns (cf. Ramsay, fig. 10–13, parts D and E), into the crescents, hearts, mushrooms and arrows that characterize many sections through Type 2 patterns. Two-dimensional patterns that are not so distinctive are simple sine waves (that occur in Types 0, 1 or 2), hooked or birdshead patterns (Types 2, 3) and straight line patterns (Types 0, 1).

CONCLUSIONS

The main modifications of Ramsay's classification of interference patterns suggested here are: (1) that a more satisfactory, though admittedly more complicated, classification requires use of at least three inter-axial angles rather than just two angles; and (2) that where only two angles are to be used, the β–γ pair is superior to the α–β pair.

Acknowledgements—We thank W. S. F. Kidd for helpful comments on the manuscript and C. Schoneveld who drew our attention to this subject by pointing out some defects of the α–β classification scheme. This paper was written while R. L. Thiessen held an N.S.F. pre-doctoral fellowship.

REFERENCES

Carey, S. W. 1962. Folding. *J. Alberta Soc. Pet. Geol.* **10,** 95–144.
Nye, J. F. 1964. *Physical Properties of Crystals.* Clarendon Press, Oxford.
O'Driscoll, E. S. 1962. Experimental patterns in superposed similar folding. *J. Alberta Soc. Pet. Geol.* **10,** 145–167.
Ramsay, J. G. 1962. Interference patterns produced by the superposition of folds of "similar" type. *J. Geol.* **60,** 466–481.
Ramsay, J. G. 1967. *Folding and Fracturing of Rocks.* McGraw-Hill, New York.
Thiessen, R. L. in press. A FORTRAN program for simulation of fold interference patterns. *Computers and Geosciences.*